

# Preliminary study of 3D large deformation modeling of the Gjerdrum 2020 sensitive clay landslide

Quoc-Anh Tran, Agnete Rogstad, Gustav Grimstad Steinar Nordal, and Gebray Habtu Alene

*Department of Civil and Environmental Engineering, Norwegian University of Science and Technology (NTNU), Trondheim, Norway*



## ABSTRACT

A quick clay slide in Gjerdrum, Norway, occurred at 4 a.m. on 30th December 2020 killing 10 people and destroying houses, roads, and other infrastructures. Approximately 1.35 million cubic meters of clay were released, a large volume liquefied, and debris was transported almost two kilometers downstream. An investigation following the slide determined that the slide was initialized in a 30-meter-high slope after 2-to-2,5-meter vertical erosion in a small creek running along the toe of the slope. After the initiation, the slide developed retrogressively in the order of 500 meters backward and sideways over a period of about 2 minutes. A conventional geotechnical slope stability analysis explains the initial slide. However, more advanced numerical tools are needed to simulate the retrogressive mechanism and the debris flow. The aim of the paper is to illustrate how the Material Point Method can capture some of the mechanisms involved from initiation until the debris comes to rest.

## RÉSUMÉ

Un glissement dans des argiles sensibles à Gjerdrum, en Norvège, s'est produit à 4 heures du matin le 30 décembre 2020, tuant 10 personnes et détruisant des maisons, des routes et d'autres infrastructures. Environ 1,35 million de mètres cubes d'argile ont été libérés, un grand volume s'est liquéfié et des débris ont été transportés sur près de deux kilomètres en aval. Une enquête après le glissement a déterminé que le glissement a été initialisé dans une pente de 30 mètres de haut après une érosion verticale de 2 à 2,5 mètres dans un petit ruisseau longeant le pied de la pente. Après l'initiation, le glissement s'est développé de manière rétrogressive de l'ordre de 500 mètres vers l'arrière et latéralement sur une période d'environ 2 minutes. Une analyse géotechnique conventionnelle de la stabilité des pentes explique le glissement initial. Cependant, des outils numériques plus avancés sont nécessaires pour simuler le mécanisme rétrogressif et l'écoulement des débris. Le but de l'article est d'illustrer comment la méthode du point matériel peut capturer certains des mécanismes impliqués depuis l'initiation jusqu'à ce que les débris s'immobilisent.

## 1 INTRODUCTION

Sensitive clay landslides are common in Scandinavia and Canada. In Norway, it has been estimated that there has been approximately one large quick clay landslide per year with a volume larger than 50.000m<sup>3</sup> since 1970 (J.S. L'Heureux, 2018). A recent example is the fatal sensitive clay landslide in Gjerdrum Norway on the 30<sup>th</sup> of December 2020 killing 10 people and destroying houses and other infrastructure.

Most sensitive clay landslides are progressive or retrogressive due to significant softening after reaching the peak strength. Improving future sensitive clay hazard and risk management requires proper modelling of how this affects the initiation and mobility of the sensitive clay landslides.

To assess the triggering of failure, limit equilibrium or finite element method can be used (Locat et al., 2013; Locat et al., 2011), but they are very limited to capture the mobility of the landslides. Previously some researcher have used depth average models (Liu et al., 2021) to study the mobility (run out) of sensitive clay landslide, by integrating the balance equations along with the depth. As these models are of fluid dynamic nature, the depth average models are unable to calculate the retrogression distance of a slide like the Gjerdrum slide. This means that

the volume of soil actually released needs to be estimated and prescribed. The flow of a given released volume of liquefied soil may then be studied.

To overcome this limitation, particle-based methods have emerged as numerical tools to analyze both the static and dynamic part of the sensitive clay landslides. Examples are the coupled Lagrangian-Eulerian method (Dey et al., 2015), Material Point Method (Tran & Solowski, 2019), and Particle Finite Element Method (Zhang et al., 2020). However, all these studies were performed as under plane strain conditions without consideration of three-dimensional effect. For natural slopes that have the complexity of soil layers and topography, two-dimensional and three-dimensional slope stability analyses can give significantly different results (Alison McQuillan, 2021). Therefore, this study aims to demonstrate the ability of the Material Point Method to perform a 3D analysis of the Gjerdrum quick clay landslide. The simulation is compared to observations from the Gjerdrum landslide, in order to understand the advantages and limitations of the proposed model. Theoretically the 3D MPM model allows us to study the initiation of the failure involving strain localization, the retrogression distances, the mobility of the liquefied soil including propagation velocities, propagation direction and distances. The question is how the simulation compares to reality.

## 2 PROBLEM DEFINITION

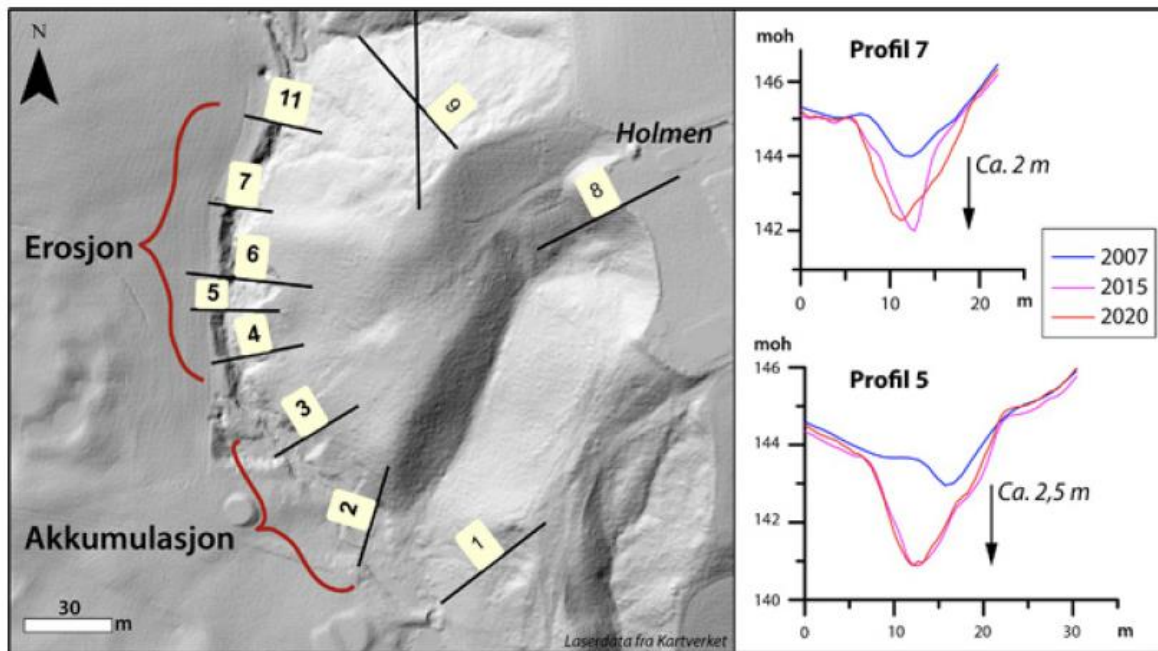


Figure 1. Erosion rate (*Årsakene til kvikkleireskredet i Gjerdrum 2020, 2021*)

There are three factors to assess the failure of a sensitive clay landslide (1) the triggering mechanism, (2) the progressive/retrogressive failure mechanism (3) the run-out mechanism. In this study, we only evaluate the first two mechanism of the Gjerdrum landslide.

Regarding the triggering mechanism in Gjerdrum landslide, the river/creek erosion in the toe of the slope seems to be the major factor causing the slide. The slide was finally triggered after heavy rain in the fall of 2020 but is believed to be brought almost to failure by the erosion. Indeed, Figure 1 shows the erosion rate from 2007 to 2020 with approximately two-meter soil layer were eroded due to the Tistilbekken creek. We also notice that the erosion between 2015 and 2020 are negligible. Therefore, the topography in 2015 may be used as the initial condition of the slide.

Regarding the progressive failure mechanism, the Gjerdrum landslide is classified as 'sensitive clay flow slide' according to the updated Varnes classification of landslide types (Hungr et al., 2014). This is a typical progressive failure mechanism in Norway with multiple shear bands propagating backwards. In terms of the mobility of a sensitive clay landslide, there are three characteristics including the propagation rate, the propagation direction, and the retrogression distances. We will examine those characteristics in this study. The Gjerdrum landslide was reported to be retrogressively released in about nine stages (see Figure 2 from (*Årsakene til kvikkleireskredet i Gjerdrum 2020, 2021*)). This conclusion is based on the interpretation of the photos, the videos, the geotechnical and hydraulic investigations, and the testimonies from witnesses.

## 3 RESEARCH METHODOLOGY

### 3.1 Hypothesis

- The erosion is the main factor to trigger the landslide. Since erosion is negligible between 2015 and 2020, the soil topography in 2015 is considered as initial ground elevation for the numerical model.
- The landslide occurred rapidly, therefore; the clay is assumed to behave in undrained condition. For the sake of simplicity, undrained parameters are obtained from representative boreholes and in literature for the entire area.
- The model does not consider several important features regarding the failure of the slope such as soil anisotropy, hydraulic conditions, weather conditions, external loading from buildings or snow.

### 3.2 Implementation

To simulate the entire process of the Gjerdrum landslide, it is required to:

- convert the digital elevation model in 2015 to the Material Point Method discretization for the numerical simulation,
- interpret soil parameters from the soil investigation,
- perform 3D numerical analysis using the Material Point Method to investigate the retrogressive failure mechanism and compare with the Gjerdrum landslide 2020 report (*Årsakene til kvikkleireskredet i Gjerdrum 2020, 2021*).

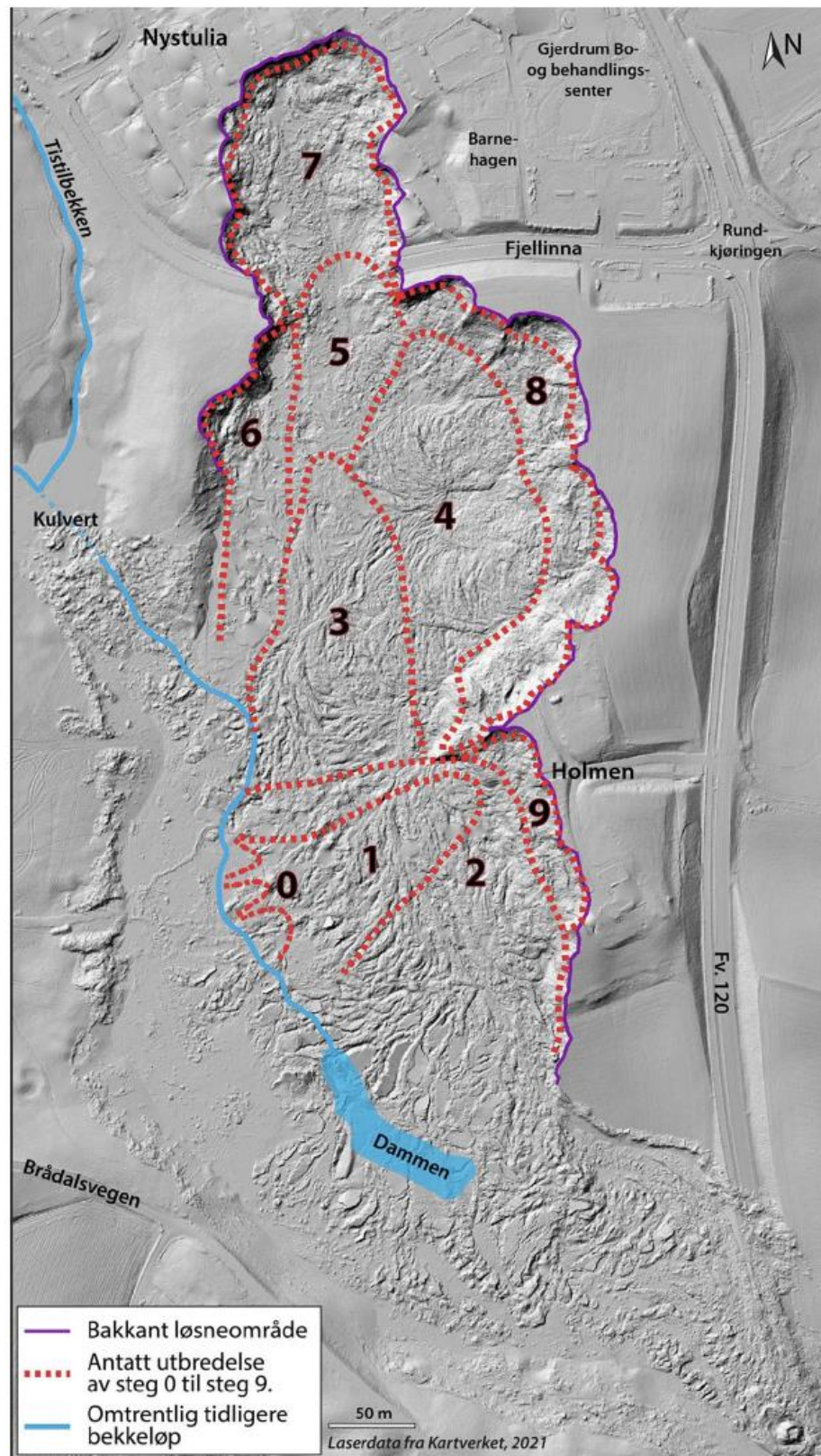


Figure 2. Assumed propagation of the slide (*Årsakene til kvikkleireskredet i Gjerdrum 2020, 2021*)  
 Purple line – ground release area, dot red line – estimated propagation of step 0 to step 9,  
 blue line - approximately previous brook run



## 4 NUMERICAL MODEL

### 4.1 Material Point Method

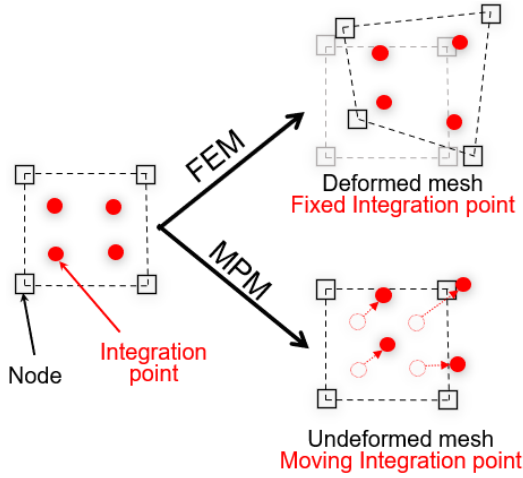


Figure 3. Comparison between FEM and MPM

Material Point Method (MPM) is a continuum-based method for the modeling of large deformations. MPM discretizes the Lagrangian particles (or integration points in FEM) in a background mesh. The differential equations in the weak form are also solved on the background mesh, as in FEM. In contrast to FEM, the solutions (e.g., deformations) are updated in particles rather than the mesh and the background mesh is reset to the reference configuration (see Figure 3). This technique refers to an updated Lagrangian formulation. The method allows large deformations to be handled, however, some numerical instability occurs when particles pass through element boundaries. In addition, arbitrary particle positions in MPM may result in larger numerical integration errors as compared to FEM. In this paper, we adopted the generalized interpolation material point method, which is more accurate and stable compared to the original MPM.

### 4.2 From Digital elevation model to 3D discretization

To reconstruct the soil topography, MPM particles are first generated from raster data of the Digital elevation model using the MPM particle discretization technique (Fernandez et al., 2020). The Digital Elevation Model has a resolution of 0.5 meters. After generating the MPM particles, the regular mesh is discretized with a resolution of one meter. Four particles are generated per element in the MPM model. A discretization procedure generates 127,366,460 particles and 32,923,168 elements for the background grid. Figure 4 shows the initial topography of the numerical model with colors indicating elevation. This shows a few quite steep slopes with an inclination of approximately 30 degrees.

### 4.3 Material behaviour of the sensitive clay

In this study, the behaviour of the clay is described by an elasto-plastic Mohr Coulomb model with a non-associated flow rule. Since the material behave in undrained condition, the friction angle is set to be zero and the model is converted to Tresca yield criteria with associated flow rule.

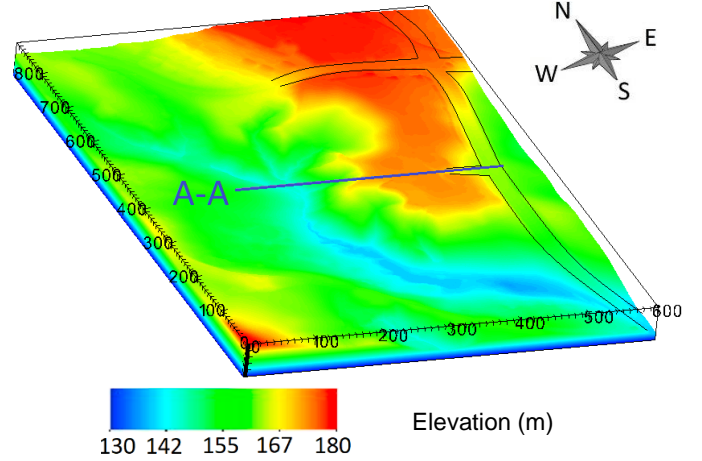


Figure 4. Initial topography of the landslide area

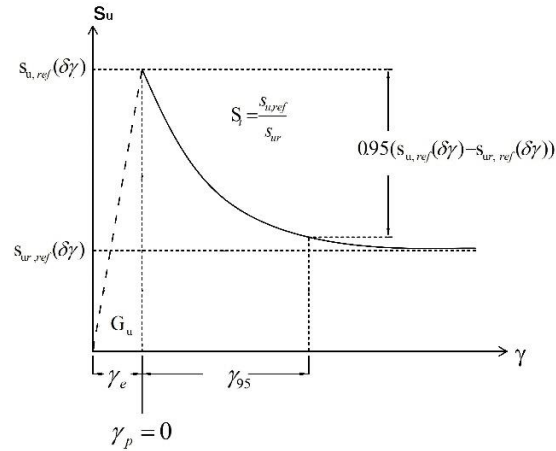


Figure 5. Constitutive model for the sensitive clay

To capture the softening behavior of the sensitive clays, the undrained shear strength decreases with the increase of the plastic shear strain (Tran & Solowski, 2019). The formula for the shear strength reduction is:

$$s_u(\gamma, S_t) = s_{u,ref} \left[ \frac{1}{S_t} + \left(1 - \frac{1}{S_t}\right) e^{-3\gamma/\gamma_{95}} \right] \quad [1]$$

where  $\gamma_{95}$  is the accumulated shear strains required to obtain 95% reduction of shear strength and the sensitivity  $S_t$  is the ratio of undisturbed over remoulded undrained shear strength.  $\gamma$  is the current accumulated shear strain. Figure 5 shows the constitutive relation between the undrained shear strength and the shear strain for the sensitive clays.

The soil properties are based on soil investigation and laboratory tests performed by Multiconsult. These soil investigations were carried out after the landslide event. The average value of the density is 19.5 kN/m<sup>3</sup> (Multiconsult, 2021a). The undrained Poisson's ratio is set to 0.49. The boreholes 2020-120 and 2020-121 (Multiconsult, 2021c) indicated that the plasticity index is between 5% and 15%. Therefore, Young's modulus is set to be 1000 times of the undrained shear strength based on the empirical relation (Duncan & Buchignani, 1976).

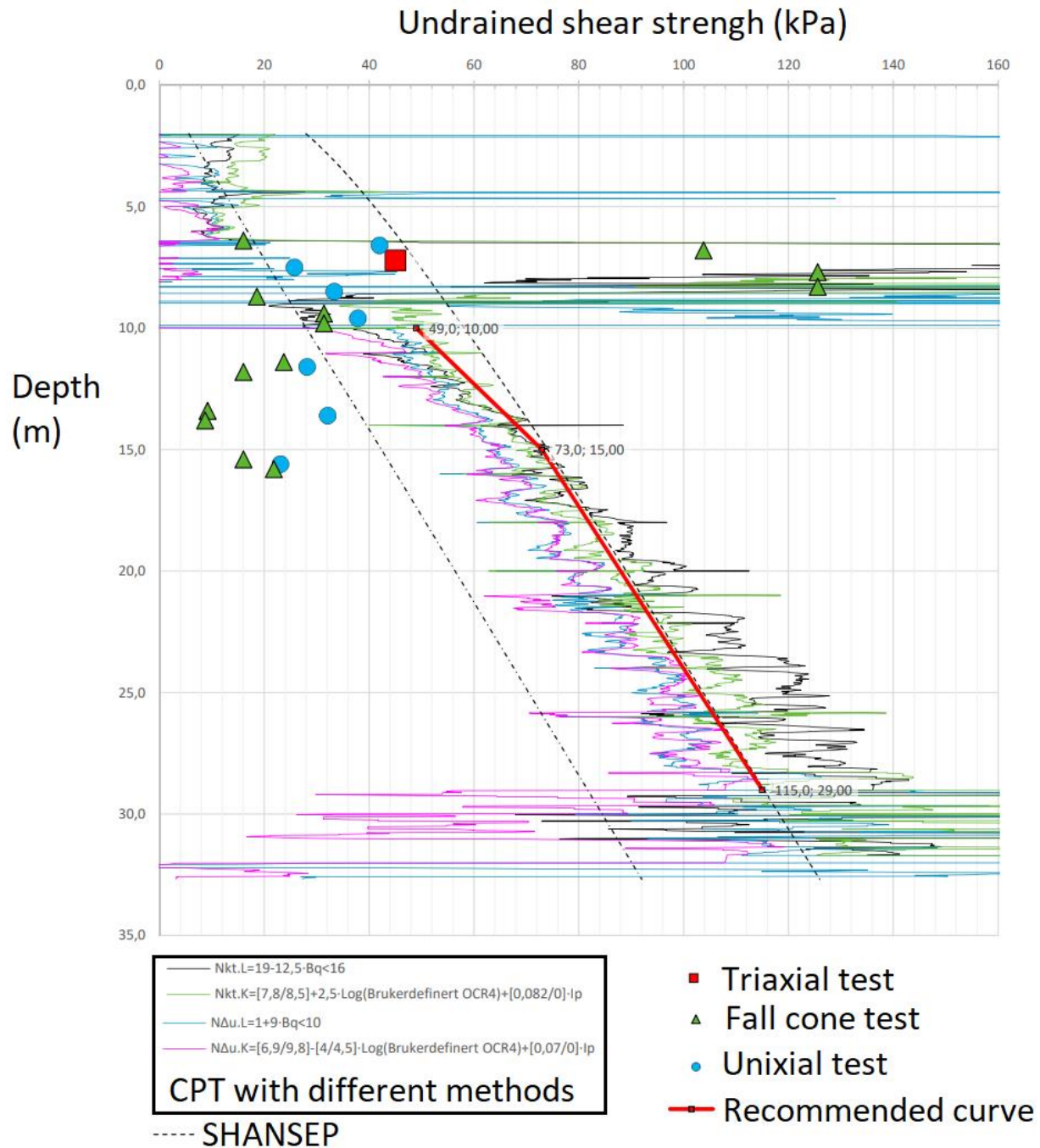


Figure 6. Undrained shear strength in cross section A-A

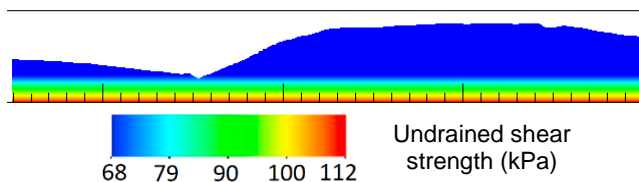


Figure 7. Undrained shear strength in cross section A-A

Based on the results from the boreholes 2020-120 (see Figure 6 for the borehole 2020-120), 2020-121, 2020-140

and 2020-138 (Multiconsult, 2021b), the soil parameters are analyzed and simplified for 3D numerical analysis (Rogstad, 2021). We also note that the undrained shear strength was adjusted upward to get the safety factor close to 1. For sake of simplicity, the undrained shear strength is set constant at 68 kPa to a reference depth and then increase linearly with depth. Below the reference depth the shear strength increase linearly with 3 kPa per meter. Figure 7 shows the variation of the undrained shear strength at the cross section A-A shown in Figure 4.

Regarding the softening behaviour, sensitivity was determined from the boreholes 2020-120 and 2020-121 (Multiconsult, 2021c). The clay sensitivity is thus assumed to be 25 as average value and the 95% remoulded shear strain to be 200%. To avoid the mesh dependency, the embedded shear band technique (Tran & Solowski, 2019) was used in this study, and we assume the thickness of the shear band is 0.2 m. This technique has been shown to minimize the mesh dependency in the MPM solution. Table 1 summarizes the parameters in the numerical simulation.

Table 1. Sensitive clay parameters for undrained model

Model Parameters	Unit	Value
Density	$\gamma$ (kN/m <sup>3</sup> )	19.5
Bulk modulus	K (MPa)	2267
Shear modulus	G (MPa)	22.74
Reference undrained shear strength	$S_u$ (kPa)	68
Increment of shear strength	$\Delta S_u$ (kPa)	3
Sensitivity	$S_t$	25
95% remoulded shear strain	$\gamma_{95}$	200%

## 5 RESULTS

The simulation is performed in the high-performance computing 'Betzy' using 12800 CPUs and it took approximately 24 hours for computing 180 seconds in the simulation with the time step  $1e^{-3}$  seconds.

In the case of simulations with no sensitivity, no failures are observed. It has also been verified by 2D finite element analysis using PLAXIS2D (Rogstad, 2021) in a 2D typical cross-section with similar soil parameters. It was shown that the sensitivity of the sensitive clays is crucial in triggering the progressive failure of the sensitive clay landslide.

A sensitivity of 25 has been assigned to the simulation in Figure 8, which shows the numerical results at 10 seconds in the elevation map. Blue indicates those clays with a shear strain greater than 200% and, therefore, have been completely remoulded. After ten seconds, the first slide began at the same location as described in the documentation for the Gjerdrum landslide (see stages 1 and 2 in Figure 2). The sensitive clay was rapidly remoulded, a similar process to liquefaction. It is evident that the remoulded clay (blue color) has a sudden change of phase, from solid to liquid, and that the slide is propagating to the northeast.

Another important characteristic of the sensitive clay landslide is the retrogression distances. In the Gjerdrum landslide, the slide developed retrogressively backward, in the order of 500 meters backward and sideways over a period of about 2 minutes. Overall, the simulation seems to overestimate the propagation rate of the landslide as it took 1 minute to propagate backward compared to 2 minutes as reported in the documentation of the Gjerdrum landslide. However, we also notice that the softening rate of the sensitive clay is the key factor controlling the propagation rate of the landslide (quantified by the parameter  $\gamma_{95}$  as 95% remoulded shear strain). This is confirmed by other studies

that show the influence of the softening rate on the propagation of the landslide (Locat et al., 2013; Locat et al., 2011).

Figure 9 and Figure 10 show a progressive failure at 30 seconds and 60 seconds respectively. Even though the propagation rate was overestimated, the propagation direction seems naturally well-captured compared to the documentation of the Gjerdrum landslide (see Figure 2). This is due to the capability of the proposed model to capture the complexity of the topography of the area. Indeed, the landslide tends to propagate towards the urban area where the elevation is highest in the numerical model.

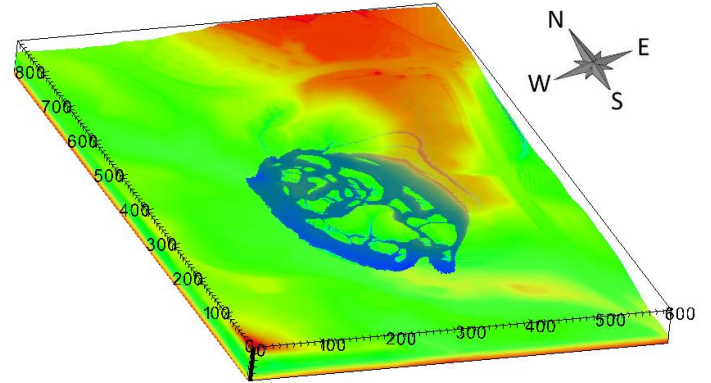


Figure 8. Progressive failure at 10s after initiation

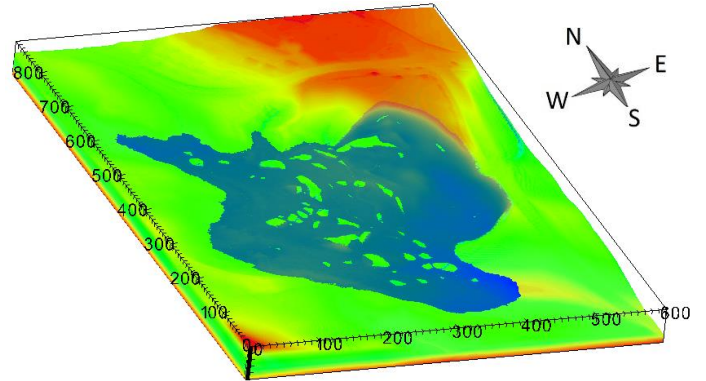


Figure 9. Progressive failure at 30s after initiation

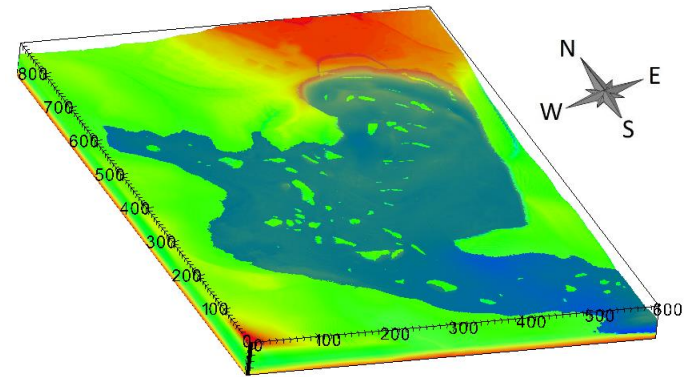


Figure 10. Progressive failure at 60s after initiation



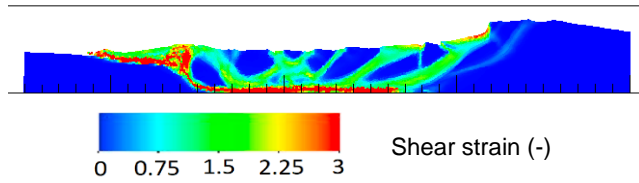


Figure 11. Shear strain color map of the cross section A-A

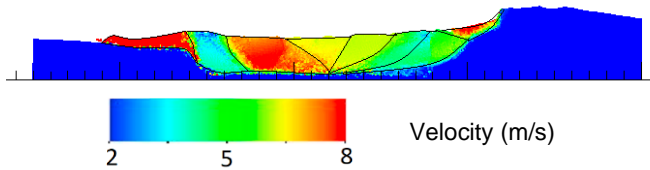


Figure 12. Velocity map (m/s) of the cross section A-A

The 3D simulations also allow taking an arbitrary cross-section out of the 3D model. For example, Figure 11 shows the shear band propagation in the cross-section A-A at 10 seconds and it shows the propagation of multiple inclined shear bands. This demonstrates the capability of the proposed method to study the failure mechanism involving strain localization. However, the shear bands in the 3D model are commonly curved, making it difficult to visualize the shear band in a 2D plot. Overall, the shear bands patterns show the sign of a sensitive clay flow slide with multiple shear band propagating upwards.

To further investigate the dynamic motion of the landslide, Figure 12 shows the value of the velocity of the cross-section A-A at 10 seconds. In general, the soils were dislocated in blocks of high undrained shear strength. In the simulation, the maximum velocity of the soil blocks is approximately 8 m/s and gradually reduces to 5 m/s backward. According to the updated Varnes classification of landslide types (Hung et al., 2014), this landslide velocity is classified as an 'extremely rapid' velocity scale and it is higher than the actual estimated velocity.

It should be mentioned that the simulations overestimated the retrogression distance of the slide to the east. This shortcoming is due to the oversimplification of the properties of the soil layer. In the simulation, the soil layer is assumed to be homogeneous with the undrained shear strength increasing linearly with depth in the entire area (see Figure 7). On the other hand, the soil investigation revealed that the soil layer is rather complex. There are two main characteristics in this area. Firstly, the level of bedrock increases gradually to the east and secondly, a non-sensitive clay layer was detected in the east of the area. It can be seen in Figure 13 which shows the soil profile of a typical cross-section. The brown color represents a very thick sensitive clay layer while the soil layer in the east was covered by a non-sensitive clay layer (green color). It is expected that a more realistic retrogression distance can be reproduced using a more realistic soil profile layer.

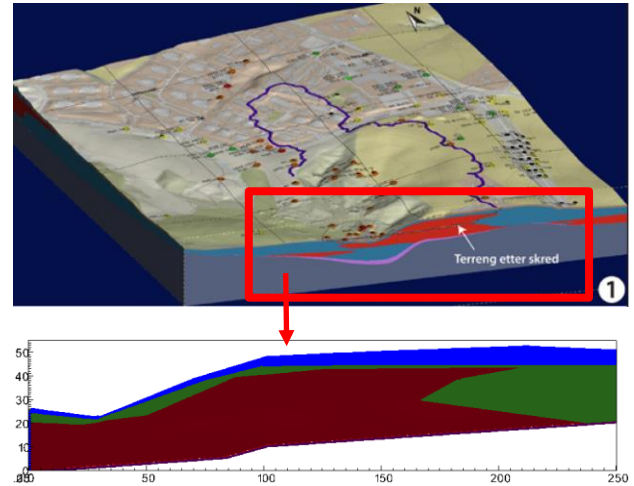


Figure 13. Soil profile (blue is crust layer, brown is quick clay, green is non-sensitive clays and white is bed rock)

## 6 CONCLUSION

The paper demonstrates the capability to model the entire process of a 3D progressive/retrogressive failure of a sensitive clay landslide. Based on the numerical analysis, we demonstrate that:

- The numerical model can capture the mobility of the Gjerdrum quick clay under the assumption that the Gjerdrum landslide is triggered by erosion near the Tistilbekken creek. The model also allows to study the failure mechanism involving strain localization.
- Large volumes of soil can progressively/retrogressively fail for the soil with high sensitivity (e.g., a sensitivity of 25 in the simulation of the Gjerdrum landslide). When the soil has no sensitivity, the slope failure was not observed in the simulation. The softening rate is a key factor to control the propagation rate. The propagation direction can be captured by considering the topography of the area using digital elevation data (a digital map).
- In our case the simulation overestimated the retrogression distance of the Gjerdrum landslide. The simple explanation for this is that we oversimplified the soil layering in the northeast part of the area. In particular, in reality, there is a non-sensitive clay layer in the east of the area which is not considered in our numerical model. Taking strongly varying soil data into account is a bit complicated and was not done in this study.

Our future research will address more realistic soil conditions, in particular considering the presence of the bedrock, crust layer and non-sensitive clay in the model. Also, spatial variability of soil properties (the undrained shear strength of clays) can be considered in the model in order to perform reliability analysis.

This model is limited by the high computational cost caused by a large number of particles and elements (127.366.460 particles and 32.923.168 elements) with a mesh size of 1 m. By increasing the mesh size, it is possible to achieve a reasonable computational cost for a standard computer, but this will lead to a reduction of numerical accuracy. Because of this limitation, such models rely upon high

performance computer, which limits their use in practice outside academia.

## 7 ACKNOWLEDGMENTS

This research received support from the European Union's Horizon 2020 research and innovation program under the grant agreement 101022007. The computations were performed on High-Performance Computing resources provided by UNINETT Sigma2 – the National Infrastructure for High-Performance Computing and Data Storage in Norway. The support from Fabricio Fernandez for 3D MPM discretization is greatly acknowledged.

## 8 REFERENCES

- Alison McQuillan, N. B., T. Yacoub. (2021). On the comparison of 2D and 3D stability analyses of an anisotropic slope. RIC2021: Rocscience International Conference, Toronto, Canada.
- Årsakene til kvikkleireskredet i Gjerdrum 2020. (2021).
- Dey, R., Hawlader, B., Phillips, R., & Soga, K. (2015). Large deformation finite-element modelling of progressive failure leading to spread in sensitive clay slopes. *Geotechnique*, 65(8), 657-668. <https://doi.org/10.1680/geot.14.P.193>
- Duncan, J., M., & Buchignani, A. L. (1976). *An Engineering Manual for Settlement Studies*. Department of Civil Engineering, University of California.
- Fernandez, F., Vargas, E. D., & Velloso, R. Q. (2020). A 3D discretization procedure for the material point method (MPM). *Computational Particle Mechanics*, 7(4), 725-733. <https://doi.org/10.1007/s40571-019-00303-7>
- Hungr, O., Leroueil, S., & Picarelli, L. (2014). The Varnes classification of landslide types, an update. *Landslides*, 11(2), 167-194. <https://doi.org/10.1007/s10346-013-0436-y>
- J.S. L'Heureux, O. A. H., A.P. Paniagua-Lopez, S. Lacasse. (2018). Impact of climate change and human activity on quick clay landslide occurrence in Norway. Second JTC1 Workshops on Triggering and Propagation of Rapid Flow-like Landslides, Hong Kong.
- Liu, Z. Q., L'heureux, J. S., Glimsdal, S., & Lacasse, S. (2021). Modelling of mobility of Rissa landslide and following tsunami. *Computers and Geotechnics*, 140. <https://doi.org/ARTN> 104388 10.1016/j.compgeo.2021.104388
- Locat, A., Jostad, H. P., & Leroueil, S. (2013). Numerical modeling of progressive failure and its implications for spreads in sensitive clays. *Canadian Geotechnical Journal*, 50(9), 961-978. <https://doi.org/10.1139/cgj-2012-0390>
- Locat, A., Leroueil, S., Bernander, S., Demers, D., Jostad, H. P., & Ouehb, L. (2011). Progressive failures in eastern Canadian and Scandinavian sensitive clays. *Canadian Geotechnical Journal*, 48(11), 1696-1712. <https://doi.org/10.1139/T11-059>
- Multiconsult. (2021a). 10226192-01-RIG-BER-001 rev00 *Teknisk beregningrapport { Parametere}* (Oslo: Multiconsult, Issue.
- Multiconsult. (2021b). 10226192-01-RIG-BER-002 *Teknisk beregningsrapport - Stabilitetsberegninger* (Oslo: Multiconsult., Issue.
- Multiconsult. (2021c). NVE Ekstern rapport nr. 13/2021 *Grunnundersøkelser i evakuerte områder i Ask sentrum etter kvikkleireskredet i Gjerdrum, 30.12.2020 : datarapport for delområde H*.
- Rogstad, A. (2021). *Gjerdrum landslide: a study of the initial slide*. Department of Civil and Environmental Engineering, Norwegian University of Science and Technology.
- Tran, Q. A., & Solowski, W. (2019). Generalized Interpolation Material Point Method modelling of large deformation problems including strain-rate effects - Application to penetration and progressive failure problems. *Computers and Geotechnics*, 106, 249-265. <https://doi.org/10.1016/j.compgeo.2018.10.020>
- Zhang, X., Wang, L., Krabbenhoft, K., & Tinti, S. (2020). A case study and implication: particle finite element modelling of the 2010 Saint-Jude sensitive clay landslide. *Landslides*, 17(5), 1117-1127. <https://doi.org/10.1007/s10346-019-01330-4>